Statistical properties and shell analysis in random cellular structures

T. Aste,* K. Y. Szeto, and W. Y. Tam

Department of Physics, The Hong Kong University of Science and Technology, Clear Water Bay, Kowloon, Hong Kong

(Received 24 April 1996)

We investigate the statistical properties of two-dimensional random cellular systems (froths) in terms of their shell structure. The froth is analyzed as a system of concentric layers of cells around a given central cell. We derive exact analytical relations for the topological properties of the sets of cells belonging to these layers. Experimental observations of the shell structure of two-dimensional soap froth are made and compared with the results on two kinds of Voronoi constructions. It is found that there are specific differences between soap froths and purely geometrical constructions. In particular these systems differ in the topological charge of clusters as a function of shell number, in the asymptotic values of defect concentrations, and in the number of cells in a given layer. We derive approximate expressions with no free parameters which correctly explain these different behaviors. [S1063-651X(96)13111-1]

PACS number(s): 82.70.−y, 68.90.+g

I. INTRODUCTION

Materials consisting of cellular structures such as metal grains and biological tissues are common in nature [1,2]. Among these systems, soap froth is considered to be the paradigm for the study of trivalent two-dimensional cellular structures. The structural analysis of two-dimensional cellular patterns has been made by many researchers and many interesting results have been obtained [3–12]. These studies of the topological properties of soap froth can be summarized in several laws such as Lewis' law [13] on the statistics of cell area, von Neumann's law [14] on the growth rate of n-sided cells, the scaling law [6] on the probability distribution of the cells, and Aboav-Weaire's law on nearest-neighbor correlation [15,16]. So far, the evolution of soap froth after the scaling state defined as stationary probability distribution of cell sides has been explained by several theories [17–20], indicating that correlation effects are not manifested in the analysis of area scaling law. However, a more detailed analysis beyond the area scaling law has been done [21] and strongly suggests the importance of clarifying the role of correlation effects. Moreover, to our knowledge, there has been no experimental investigation until recently [22] on the statistical properties and correlation effects beyond nearest neighbors in two-dimensional soap froth. With the advance of experimental techniques and data analysis [23,24,22], it is natural to investigate the structural characteristic of soap froth beyond nearest neighbors. Here we derive systematically exact expressions for the topology of the froth structure beyond first neighbors. Our results will serve as a mathematical framework for our data analysis, which enhances our ability to test current theoretical ideas and our understanding of topological ordering processes in soap froth [25–29]. Our aim is to extract more information about the differences between physical soap froths and computer generated two-dimensional cellular patterns, such as the Voronoi construction of points randomly scattered on the plane.

Soap froths are trivalent (three edges meeting at a vertex) two-dimensional cellular patterns. Any two-dimensional (2D) froth can be analyzed as being structured in concentric layers of cells around a given central "germ" cell [25,30,22]. The first layer of the shell structure consists of neighbors of the germ cell, the cells of the second layer are the neighbors that externally bound the first layer, etc. (see Fig. 1). More precisely, the layers are closed rings of cells which are at the same topological distance from the germ cell (the topological distance between two cells is defined as the minimum number of edges that a path must cross to
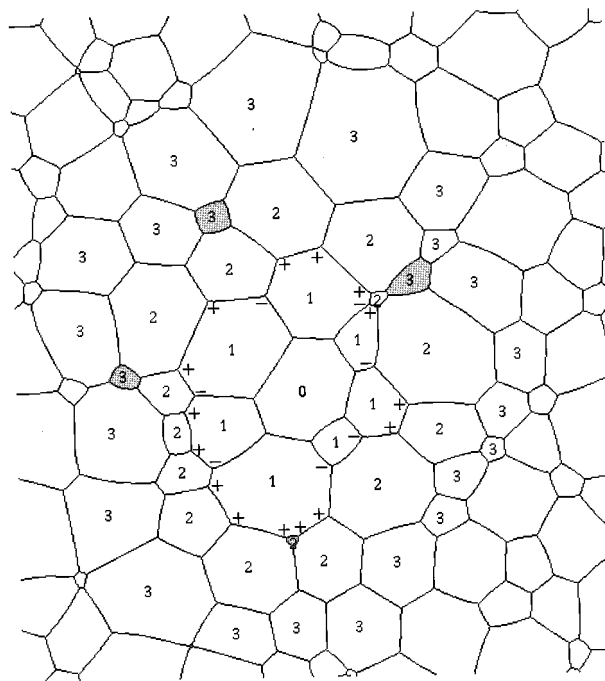
FIG. 1. Shell structure and defects in trivalent two-dimensional froth. The defects are shaded and the number denotes the topological distance from the center cell labeled O, which is a deformed heptagon.

*Present address: Laboratorie the Physique Théorique, Université Louis Pasteur, Strasbourg, France.

connect these two cells). The shell is a closed loop of edges which are the interface between two subsequent layers (see Fig. 1). (The definition here is consistent with Ref. [30]. Note that in our previous work [22], the word ''shell'' is used to indicate the layer used in this paper.)

The shell structure has some physical relevance in natural froths and in problems of the topologically stable partition of space by cells. In foams the evolution of the cellular structure is ruled by the process of diffusion of the gas inside a given bubble toward its neighbors. The topological distance j between two cells is the minimum number of soap membranes that the gas molecules have to cross to pass from one cell to the other. The molecules which diffuse from a given central bubble move through the shell structure, reaching the cells of each layer with an approximately equal probability. An analogous problem where the shell structure has physical relevance is the random walk through a barrier network. In this case the topological distance j is the minimum number of barriers that must be crossed from a starting cell to a given final cell. The number of cells in the layer j is the number of final states with approximately equal probabilities. More generally, any perturbation on a given cell (cell growth, cell division, mechanical stress, cell coalescence, electrical signal, etc.) propagates in the whole system through the shell network, and reaches with approximately equal intensity all cells at the same topological distance from the perturbed cell at about the same time. These considerations provide the motivation for introducing shell structure analysis for froth.

The quantities investigated for a shell at topological distance j from a given n-sided germ cell are the total number of cells in the layer (K_j), the average number of sides of the cells belonging to the layer (m_j), and the topological charge (Q_j) of the cluster of cells delimited by the shell j. Here, the topological charge of a cell with n sides is defined as $q = 6 - n$ and Q_j is defined as the sum over the topological charges of all the cells inside the cluster delimited by the shell j which separates the layer j from the layer $j + 1$. Note that all these quantities K_j, m_j, and Q_j can depend on n.

The experimental investigation of the statistical properties of natural and computer generated froths in terms of the shell structure gives some interesting results. For instance, we find that the number of cells in a layer at a topological distance j from the germ cell increases with distance following a linear law $K_j = Cj + B$ with slope $C \sim 9$ (see also Ref. [22]). This is in contrast to simple geometrical considerations that the perimeter of the shell cluster increases with the radius with a slope of approximately 2π. Moreover, we find that the topological charge of the cluster bounded by the shell j is negative, and decreases linearly with j. This behavior is particularly surprising since the total topological charge of a froth is a constant finite quantity independent of the network itself, and is related to the space curvature by the Euler formula associated with the Gauss-Bonnet theorem [31,32]. Therefore, the set of cells belonging to a layer has peculiar statistical properties which are different from the one for the whole froth. The aim of the present paper is to study these peculiarities with an exact analytical approach, and to find approximate solutions with no adjustable parameters which can be compared with the experimental observations.

The plan of the paper is as follows. In Sec. II, we derive the statistical properties of the shell structure for a special class of froths called shell-structured-inflatable (SSI) froths [30]. These froths are particularly convenient since they can be constructed layer by layer in a recursive way according to an inflationary procedure. In Sec. III, we study the correlation length in SSI Euclidean froths. Approximate expressions for K_j and Q_j are also derived. In Sec. IV, the results obtained for SSI froths are generalized to non-SSI systems. In Sec. V, we find approximate expressions for K_j and Q_j in the general case of non-SSI froths. In Sec. VI, experimental results are presented and compared with analytical predictions. Section IV contains a conclusion that emphasizes the main results. In Appendix A, a generalization of Weaire's sum rule [16] is derived. In Appendix B, we find an expression for the fluctuations of the topological charge. Finally, in Appendix C, a proof of the correlation theorem of euclidean SSI froth is given.

II. STATISTICAL PROPERTIES IN SHELL-STRUCTURED-INFLATABLE FROTHS

Any froth can be analyzed as structured in concentric layers of cells which are at the same topological distance from a given central cell. These concentric layers are the shell structure of the froth. In this structure the cells forming the layer j can be divided into two categories. Some cells simultaneously have neighbors in the layers $j - 1$ and $j + 1$. These cells make themselves closed layers and constitute the ''skeleton'' (sk) of the shell structure. Other cells (or clusters of cells) are inclusions between the layers of the shell skeleton (they have neighbors in the layer $j - 1$ or other topological inclusions but not in the layer $j + 1$). The shell skeleton is itself a space-filling froth hierarchically organized around the germ cell. Once a germ cell is chosen, the shell structure and its skeleton are univocally defined, but different germ cells generate different skeletons. We call a froth shell-structured inflatable if it is free of topological inclusions. (In this paper these inclusions are also called topological defects.) For SSI froths the shell structure and its skeleton coincide.

In this section we analyzed only SSI systems (no topological defects); the results obtained for such a class of systems are extendible to froths with topological defects. The advantage of studying SSI froths is that in these systems the shell structure can be constructed by using an inflationary recursive process. In particular, one finds that the number of vertices in successive shells is related by the following map [30]:

$$\begin{pmatrix} V_j^+ \\ V_j^- \end{pmatrix} = \begin{pmatrix} s_j & -1 \\ 1 & 0 \end{pmatrix} \begin{pmatrix} V_{j-1}^+ \\ V_{j-1}^- \end{pmatrix}, \tag{1}$$

where $s_j = m_j - 4$, and m_j is the average number of sides per cells in layer j. The quantity V_j^+ (V_j^-) is the number of vertices attached to edges directed outward from shell j (directed inward to shell j) (see Fig. 1). The matrix equation (1) is the logistic map [34]. It is a dynamical map from the central germ cell ($j = 0$) to the whole froth.

Since our 2D froth is trivalent (three edges meeting at one vertex), the number of cells in layer j is $K_j = V_j^-$. In terms of these quantities Eq. (1) can be written as a recursive equation

$$K_{j+1} = s_j K_j - K_{j-1}. \tag{2}$$

The initial conditions are $V_0^- = K_0 = 0$ and $V_0^+ = K_1 = n$ is the number of neighbors of the central germ cell.

Given the set of parameters $\{s_j\}$, the solutions of Eqs. (1) or (2) are particular trajectories in the plane (j, K_j). When s_j is equal to a constant s, one finds that the parameter s separates the map into different classes [30]. Values $|s| < 2$ are associated with the elliptic region which has bounded, finite trajectories. The region $s > 2$ is the hyperbolic region associated with exponential trajectories. The point $s = 2$ divides the elliptic region from the hyperbolic region, and corresponds to tilings of the Euclidean plane. In this case one finds that the solutions are linear trajectories $K_j \propto j$. In general, when s depends on j, one can note that bounded trajectories always correspond to froths which are tiling elliptic manifolds, whereas unbounded trajectories which grow faster than j correspond to tilings in hyperbolic manifolds. The Euclidean space has trajectories between these solutions associated with spaces of opposite curvatures. They are unbounded trajectories which grow asymptotically as a linear law ($K_j \propto j$).

One finds that the total topological charge of a cluster of cells bounded by the shell j can be written in terms of numbers of vertices coming into and going out from the shell j,

$$Q_j = \sum_i (6 - n_i) = 6 - V_j^+ + V_j^-, \qquad (3)$$

where the sum runs over all the cells i in the cluster and n_i is the number of sides of the cell i [35]. Equation (3) is a general expression (valid also for non-SSI systems). It states that the total topological charge inside a cluster depends only on its boundary. For SSI froths, Eq. (3) can be rewritten as

$$Q_j = 6 - K_{j+1} + K_j. \qquad (4)$$

The inverse of this equation provides a relation between the number of cells in the layer j and the topological charge of the cells inside the cluster delimited by the shell j,

$$K_j = 6j - \sum_{i=0}^{j-1} Q_i = 6j - 6 + n - \sum_{i=1}^{j-1} Q_i, \qquad (5)$$

where we define $Q_0 = 6 - n$. Let us now make use of these recursive relations in order to evaluate the quantities K_j, Q_j, and m_j in the shell structure.

A. First shell: The Aboav-Weaire law

Consider a shell structure around an n-sided germ cell. The number of cells constituting the first layer ($j = 1$) is

$$K_1 = n, \qquad (6)$$

and the topological charge inside the cluster delimited by the first shell is by definition

$$Q_1 = (6 - n) + (6 - m_1) K_1. \qquad (7)$$

Using the sum rule (46) (see Appendix A), one obtains the average value

$$\langle Q_1 \rangle = -\mu_2, \qquad (8)$$

with $\mu_2 = \langle (n-6)^2 \rangle$. Here the averages $\langle () \rangle$ are over the cell-side distribution: $\langle () \rangle = \Sigma_n p(n)()$, with $p(n)$ being the probability of an n-sided cell in the whole froth. One can introduce the fluctuation part of topological charge Q_1 as its deviation from the average value: $\Gamma_1 \equiv Q_1 - \langle Q_1 \rangle$, where a priori the fluctuation part can be any function of n satisfying the condition $\langle \Gamma_1 \rangle = 0$. In terms of the fluctuation, the charge Q_1 can be written as

$$Q_1 = (6 - n) + (6 - m_1)n = -\mu_2 + \Gamma_1. \qquad (9)$$

Equation (9) gives the relationship between the number of sides (n) of a given germ cell and the average number of sides (m_1) of the cells neighboring this n-sided cell. In literature, such a relation has been widely studied since Aboav empirically found the linear law: $(m_1 - 6)n = \mu_2 - a(n - 6)$ [15]. One can see immediately that Aboav-Weaire's law is obtainable from Eq. (9) by imposing a linear form for the fluctuation part [i.e., $\Gamma_1 = \epsilon_1(6 - n)$, with $\epsilon_1 = 1 - a$]. This linear dependence can be interpreted in terms of the screening of the central charge $Q_0 = 6 - n$ by the charges of the first layer. The total screening charge in the first layer is $(6 - m_1)n$ and its deviation from the average is

$$(6 - m_1)n - \langle (6 - m_1)n \rangle = -a(6 - n). \qquad (10)$$

We can therefore interpret a as a screening factor: $a = 1$ corresponds to a total screening of the internal charge, whereas $a = 0$ corresponds to absence of screening.

Aboav-Weaire's law is generally associated with the presence of topological correlations between nearest-neighbor cells. In Appendix B we discuss in detail the effects of finite range correlations in froths. Let us note that an arrangement of cells free of correlation (called a topological gas [36]) has $m_1 = 6 + \mu_2/6$ [37], which leads to an Aboav coefficient $a = -\mu_2/6$, and m_1 is independent of n.

B. Generic j shell

The average topological charge inside the cluster delimited by shell j is

$$\langle Q_j \rangle = \sum_{i=1}^{j} \langle (6 - m_i) K_i \rangle. \qquad (11)$$

Indeed, the topological charge is an additive quantity and therefore $\langle Q_j \rangle$ is the sum of the topological charges contained in the layers i ($\langle (6 - m_i) K_i \rangle$) which are inside the cluster with radius j ($i \leq j$). As before, we introduce the fluctuations of the topological charge in a cluster

$$\Gamma_i = Q_i - \langle Q_i \rangle. \qquad (12)$$

By using the generalized Weaire identity $\langle (6 - m_j) K_j \rangle = \langle (6 - n) K_j \rangle$ [Eq. (A2) in Appendix A] and by substituting Eq. (5) into Eq. (11), we can express the portion of charge contained inside the layer j in terms of the topological-charge fluctuations

$$\langle (6 - m_j) K_j \rangle = -\mu_2 - \sum_{i=1}^{j-1} \langle (6 - n) \Gamma_i \rangle = -\sum_{i=0}^{j-1} \langle (6 - n) \Gamma_i \rangle, \qquad (13)$$

where we used $\Gamma_0 \equiv (6-n)$. The total charge of the cluster inside the shell j is therefore

$$\langle Q_j \rangle = -\mu_2 j - \sum_{i=1}^{j-1} (j-i)\langle (6-n)\Gamma_i \rangle$$

$$= -\sum_{i=0}^{j-1} (j-i)\langle (6-n)\Gamma_i \rangle. \qquad (14)$$

Note that, in the absence of fluctuations ($\Gamma_i = 0$ for $i > 0$), Eq. (13) gives a topological charge per layer equal to $-\mu_2$, and therefore a total charge which decreases linearly in j with slope $-\mu_2$.

Using Eq. (14) and the definition of Γ_j, one can rewrite Eq. (5) in terms of the fluctuations

$$K_j = 6j - \sum_{i=0}^{j-1} Q_i$$

$$= 6j - (6-n) - \sum_{i=1}^{j-1} Q_i$$

$$= 6j + n - 6 + \frac{j(j-1)}{2}\mu_2 - \sum_{i=1}^{j-1} \Gamma_i$$

$$+ \sum_{i=1}^{j-2} \frac{(j-i)(j-i-1)}{2}\langle (6-n)\Gamma_i \rangle$$

$$= 6j - \sum_{i=0}^{j-1} \Gamma_i + \sum_{i=0}^{j-2} \frac{(j-i)(j-i-1)}{2}\langle (6-n)\Gamma_i \rangle.$$

$$(15)$$

These relations for K_j, Q_j, and m_j are exact results valid for any SSI froth. The fluctuations Γ_j are *a priori* unknown functions subjected to the constraint $\langle \Gamma_j \rangle = 0$. Other constraints on these fluctuations come from the space-filling condition.

III. SHELL STATISTIC OF EUCLIDEAN FROTHS

Let us consider a Euclidean 2D froth. In such a froth the number of cells per layer must grow linearly with the distance in the asymptotic limit. We will show that fluctuations in the topological charge ($\Gamma_j \neq 0$) are essential for filling space with disordered ($\mu_2 \neq 0$) Euclidean SSI cellular systems. Consider a system with $\Gamma_i = 0$ for $i \geq 1$ (recall $\Gamma_0 = 6-n$), from the next to last equality of Eq. (15), one obtains that the number of cells in the generic layer j increases quadratically with the distance $K_j \propto j^2 \mu_2$. Such a froth is realizable only in a space with intrinsic dimension $D = 3$ and thus it is not two-dimensional Euclidean. In natural froths and in computer-generated cellular system the shell structure is organized in order to keep the froth Euclidean, and experimentally one finds that the number of cells per layer increases linearly in j after the first few layers [22]. Such organization can be provided by the Γ's, which must be different from zero at least for the first few shells.

We have the following interesting theorems (see Appen-

dix C for a proof.) For a Euclidean SSI froth with $\mu_2 \neq 0$ that obeys Aboav-Weaire's law, cells must be correlated at least between the third neighbors. This theorem can be restated into two parts: (1) If a Euclidean SSI froth with nonzero second moment obeys Aboav-Weaire's law, the minimum ν in order that $\langle K_j \rangle \propto j$ for $j \geq \nu$ is 3. (2) Under the same hypothesis as (1), and if the topological correlations vanish after the ξth layer, then $\xi \geq \nu$. Therefore, (2) also means that $\xi \geq 3$. An important point in the theorem is that the Aboav parameter a is a free parameter, for otherwise, we can have an even smaller ν. (Indeed, if we restrict a to 1, then $\nu = 1$, and if we restrict a to 2, then $\nu = 2$, and if we do not put any restriction on a, then $\nu \geq 3$.) Next we will explore some consequences of this theorem.

For a space-filling Euclidean froth where the correlation length is minimal ($\xi = \nu = 3$) and Aboav-Weaire's law is satisfied with $\Gamma_1 = (1-a)(6-n)$, Eq. (C3) implies $(1-a)\mu_2 + \langle (6-n)\Gamma_2 \rangle = -\mu_2$. A solution for this condition is given by $\Gamma_2 = (a-2)(6-n)$. Since we have $\xi = \nu = 3$, we can set $\Gamma_j = 0$ for $j \geq 3$ [from Eqs. (C3) and (B3)]. With these values of Γ_j, we can work out the solution for the number of cells per layer,

$$K_1 = n, \quad K_2 = 12 + \mu_2 + (2-a)(n-6),$$

$$K_j = (6 + (3-a)\mu_2)j - (5-2a)\mu_2 \text{ for } j \geq 3. \qquad (16)$$

and the topological charge

$$Q_1 = -\mu_2 + (1-a)(6-n),$$

$$Q_2 = -(3-a)\mu_2 + (a-2)(6-n),$$

$$Q_j = -(3-a)\mu_2 \text{ for } j \geq 3. \qquad (17)$$

The solution Eq. (16) for the trajectories K_j is qualitatively in agreement with the experimental data. The number of cells per layer versus j follows a linear law with slope $6 + (3-a)\mu_2$ and intercept $-(5-2a)\mu_2$. Assuming typical values $a \simeq 1$ and $\mu_2 \simeq 1.5$, we obtain 9 and -4.5, respectively, for the typical slope and intercept. Note that a simple geometrical approach will suggest a linear growth of the number of cells of the perimeter of the shell cluster with a slope equal to about 2π, which differs from the one we have found.

Equation (17) predicts that in SSI minimally correlated froths the topological charge is constant after the second shell. This is in contradiction to the experimental data which show topological charges decreasing linearly with j. To resolve this contradiction with experimental data, we can consider the following scenario. If we take the fact that $Q_j \propto j$ for large j, then Eq. (5) implies that $K_j \propto j^2$. But our experimental froth is Euclidean with $K_j \propto j$. Thus the only possible way to resolve this contradiction to experimental data without invoking the results on a non-SSI Euclidean froth is to conclude that the assumption that $\xi = \nu = 3$ in the above analysis is incorrect. Thus this conclusion, which insists on using the results of a SSI Euclidean froth, leads one to suspect that topological correlation has a longer range: $\xi > 3$. However, this is actually misleading, as we have no good reason to insist on the assumption that the real froth is SSI Euclidean. Indeed, we have enough evidence that the real froth is a

non-SSI Euclidean froth, so that the topological correlation can vanish rather early, and still $K_j \propto j$ and $Q_j \propto j$ for large j. This point is also valid for a computer-generated froth. In Sec. IV we show that the topological defects provide a mechanism which correctly gives the behavior of the topological charge and the slope in the linear law of the trajectories K_j.

IV. EFFECTS OF THE NONINFLATABLE INCLUSIONS

The ideas presented in preceding sections for shell-structured froths are still applicable when we have noninflatable inclusions. In this section, we indicate the appropriate corrections. We use the symbols n, K_j, Q_j, m_j, and μ_2 to indicate the quantities associated with the global froth (shell skeleton plus topological inclusions) and we use the notation K_j^{sk}, Q_j^{sk}, and m_j^{sk} for the quantities associated with the shell skeleton only. Finally, we use K_j^d and m_j^d to indicate the number of defective cells and their average number of sides. Note that $K_0^d = 0$ always (since any cell of the froth can be the germ cell). One has the simple relation

$$K_j = K_j^{sk} + K_j^d. \tag{18}$$

In the general case when noninflatable inclusions are present, the relations previously obtained for the SSI froth are applicable to the quantities associated with the shell skeleton. In particular, relations (4) and (5) become

$$Q_j^{sk} = 6 - K_{j+1}^{sk} + K_j^{sk} \tag{19}$$

and

$$K_j^{sk} = 6j - \sum_{i=0}^{j-1} Q_i^{sk}. \tag{20}$$

On the other hand, expression (3) for the total topological charge of the cluster delimited by shell j remains unchanged:

$$Q_j = 6 - V_j^+ + V_j^-; \tag{21}$$

here the quantities Q and $V^{\pm}$ are associated with the global froth (shell skeleton plus topological inclusions). This equation is the topological analog of the Gauss theorem of electrostatic. The charge (topological) inside a region of space is associated with the net flux (of edges) which crosses the external surface (shell). In the absence of topological inclusion (the SSI case) the flux of edges between two adjacent shells is uninterrupted (any edge outgoing from shell j ends in shell $j+1$, i.e., $V_{j+1}^- = V_j^+$). In the general case, the topological inclusions trap the edge fluxes, and the previous identity must be modified as follows:

$$V_{j+1}^- = V_j^+ - \eta_{j+1} K_{j+1}^d, \tag{22}$$

where η_{j+1} is the average number of edges which are trapped by one defect in the layer $j+1$. One can easily verify that $V_j^- = K_j^{sk}$. By substituting Eq. (22) and V_j^- into Eq. (21), one obtains

$$Q_j = 6 - K_{j+1}^{sk} + K_j^{sk} - \eta_{j+1} K_{j+1}^d, \tag{23}$$

which is the generalization of Eq. (4). By substituting Eq. (19) into Eq. (23), one obtains

$$Q_j = Q_j^{sk} - \eta_{j+1} K_{j+1}^d. \tag{24}$$

Therefore, the topological charge inside shell j is equal to the charge associated with the shell skeleton minus a contribution due to defects attached to the external shell. This implies the important fact that defects inside the cluster do not contribute to the total charge. Moreover, note that the defects attached to the external shell always decrease the topological charge in the shell with respect to the value associated with the shell skeleton.

A. First shell and Aboav-Weaire's law

The number of cells making the first layer around an n-sided central cell is $K_1 = n$. By using the sum rule (A2) obtained in Appendix A, one can calculate the average topological charge inside the first shell:

$$\langle Q_1 \rangle = \langle (6-n) \rangle + \langle (6-m_1)K_1 \rangle = \langle (6-n)n \rangle = -\mu_2. \tag{25}$$

From this relation and Eq. (24), it follows that $\langle Q_1^{sk} \rangle = -\mu_2 + \langle \eta_2 K_2^d \rangle$.

As in the SSI case, one can introduce fluctuations of the topological charge around its average value,

$$\Gamma_j = Q_j - \langle Q_j \rangle. \tag{26}$$

In terms of these fluctuations and using Eq. (25), the charge contained in the first layer can be written as

$$Q_1 = (6-n) + (6-m_1)K_1 = -\mu_2 + \Gamma_1. \tag{27}$$

This equation gives a relation between the number of sides (n) of a given cell and the average number of sides (m_1) of the cells surrounding this n-sided cell. In the particular case that the fluctuation is linear in n, $\Gamma_1 = (1-a)(6-n)$, we arrive at Aboav-Weaire's law (i.e., $nm_1 = (6-a)n + \mu_2 + 6a$ [15]). Aboav's coefficient a can be interpreted (see Sec. II A) as the factor that represents the screening of the central charge due to the surrounding cells. By following this interpretation one can associate $a=1$ with a total screening, and $a=0$ with the absence of screening. A typical value for this coefficient in natural cellular structures (soap froth, alumina cuts, etc.) is $a \simeq 1.2$; values around 0.6 are characteristic of Voronoi froths constructed from Poissonian points, whereas random network generated by performing $T1$ transformations on regular lattice have negative Aboav's coefficients $a \simeq -1$.

B. Generic j shell

The average value of the topological charge inside the layer j can be calculated by using the sum rule (A2) [i.e.,

$\langle(6-m_j)K_j\rangle=\langle(6-n)K_j\rangle$; see Appendix A], and the expression (20) for Q_j^{sk} to obtain

$$\langle(6-m_j)K_j\rangle=\langle(6-n)K_j^d\rangle+\langle(6-n)K_j^{sk}\rangle$$

$$=\langle(6-n)K_j^d\rangle-\sum_{i=0}^{j-1}\langle(6-n)Q_i^{sk}\rangle$$

$$=\langle(6-n)K_j^d\rangle-\sum_{i=0}^{j-1}(\langle(6-n)Q_i\rangle$$

$$+\langle(6-n)\eta_{i+1}K_{i+1}^d\rangle)$$

$$=\langle(6-n)K_j^d\rangle-\sum_{i=0}^{j-1}(\langle(6-n)\Gamma_i\rangle$$

$$+\langle(6-n)\eta_{i+1}K_{i+1}^d\rangle). \tag{28}$$

The average total charge of the cluster inside shell j is the sum over the charge of individual layers. From Eq. (28) it follows that

$$\langle Q_j\rangle=\sum_{i=0}^{j-1}[\langle(6-n)K_{i+1}^d\rangle-(j-i)(\langle(6-n)\Gamma_i\rangle$$

$$+\langle(6-n)\eta_{i+1}K_{i+1}^d\rangle)]. \tag{29}$$

In this expression, the $i=0$ term is $\langle(6-n)K_1^d\rangle-j(\mu_2+\langle(6-n)\eta_1K_1^d\rangle)$, since $\Gamma_0=6-n$. From Eq. (20), using Eq. (29) and the definition of Γ_i, the number of cells of the shell skeleton in the layer j is

$$K_j^{sk}=6j-\sum_{i=0}^{j-1}Q_i^{sk}=6j-\sum_{i=0}^{j-1}(Q_i+\eta_{i+1}K_{i+1}^d)$$

$$=6j-\sum_{i=0}^{j-1}(\Gamma_i+\langle Q_i\rangle+\eta_{i+1}K_{i+1}^d)$$

$$=6j-\sum_{i=0}^{j-1}(\Gamma_i+\eta_{i+1}K_{i+1}^d+(j-i)\langle(6-n)K_i^d\rangle)$$

$$+\sum_{i=0}^{j-2}\frac{(j-i)(j-i-1)}{2}(\langle(6-n)\Gamma_i\rangle$$

$$+\langle(6-n)\eta_{i+1}K_{i+1}^d\rangle). \tag{30}$$

This is the generalization of Eq. (15) which takes into account noninflatable inclusions. These relations have the beauty of being exact and the privilege of being useless for predicting properties of real space-filling cellular systems. In order to compare with experiments, we must use some simple physical approximations that will provide predictions for the asymptotic behaviors of K_j and Q_j, and the percentage of defects.

V. EUCLIDEAN FROTHS AND NON-SSI INCLUSIONS

In the absence of defects and fluctuations, Eq. (30) implies that the number of cells in each layer grows very fast ($K_j\propto j^2$). In principle, such a fast growth is realizable in the 2D plane by increasing continuously the roughness of the cluster surface, enlarging the available space for additional cells in the layer. In practice, after some layers the rough surface of the cluster starts to self-intersect, thereby generating non-SSI inclusions (topological defects in the shell structure). These inclusions of defective cells provide a way to smooth the shell surface and to keep the froth Euclidean as a consequence. Therefore, the defects play a very important role in the froth organization.

Soap froths and computer-generated random cellular systems show asymptotically a linear increment in the number of cells per layer with the distance from the germ cell. Let us therefore consider a Euclidean froth where $K_j\propto j$ for any $j\geq\nu$. In contrast to the SSI case, when we have defects, this condition of linear growth of K_j does not introduce any constraint on the fluctuations Γ_j. Indeed, the number of defects K_j^d is a free parameter that the system can adjust in order to control the fluctuations in the topological charge and simultaneously keep the froth Euclidean. Analogously, the defects can play an important role in the reduction of topological correlations. In Sec. III we found that a SSI Euclidean froth which satisfies Aboav-Weaire's law must be correlated at least between third neighbors. The defects enlarge the freedom for the construction of the cellular system around the germ cell by removing the constraints on the fluctuations. (Without these constraints on the fluctuations, one can construct a Euclidean froth which satisfies the Aboav-Weaire law and which is correlated only between first neighbors.) Therefore the presence of defects can strongly reduce the correlations.

Consider a froth which is minimally correlated and compatible with Aboav-Weaire's law with a free a parameter. From Eq. (B3) (see Appendix B) it follows that such a froth can be uncorrelated after the first neighbors ($\xi\geq1$). (Indeed, for the topological gas, $\xi=0$ and this corresponds to $a=-\mu_2/6$.) In this case, using Eq. (30) and $\Gamma_1=(1-a)(6-n)$, one obtains

$$K_2=12+\mu_2+(2-a)(n-6)-\eta_1K_1^d+(1-\eta_2)K_2^d$$

$$+\langle(n-6)(1-\eta_1)K_1^d\rangle. \tag{31}$$

Transcurating the contribution from the defects in the first layer ($K_1^d\ll1$) and fixing $\eta_2=1$, Eq. (31) becomes

$$K_2\simeq12+\mu_2+(2-a)(n-6). \tag{32}$$

Equation (B3) gives

$$\Gamma_2=\left(1-a+\frac{(2-a)^2\mu_2}{12+\mu_2}\right)(6-n). \tag{33}$$

By using Eq. (30), one has

$$K_3\simeq18+(4-a)\mu_2+\left(3-2a+\frac{(2-a)^2\mu_2}{12+\mu_2}\right)(n-6)-K_2^d, \tag{34}$$

where we used the same approximations as for Eq. (32) plus the hypothesis $\eta_3=1$.

These relations are derived using the assumptions that $K_1^d\ll1$, $\xi=2$, and $\eta_2=\eta_3=1$. The first condition $K_1^d\ll1$ is

quite reasonable; as it is experimentally in real or computer-generated froth, the first few shells have a small number of defects. The second condition is a condition working on the conventional wisdom that the froth has rather short range correlations. In any case, this is a working hypothesis for deriving Eqs. (32), (33), and (34), which are all equations needed for comparison with experimental data in Sec. VI. As for the third condition $\eta_2 = \eta_3 = 1$, this is actually a reasonable assumption as η_{j+1} is the average number of edges which are trapped by one defect in the layer $j+1$, and many defects contribute in general only one extra edge to the correction in the defining Eq. (22).

Asymptotic behavior in Euclidean froths

In a Euclidean 2D froth, the space-filling condition implies that in the asymptotic limit the number of cells per layer grows linearly with the topological distance and, consequently, at each layer this number is incremented by a constant amount. In a froth where the cells are uncorrelated after a given topological distance ξ, this rate of increment must be a constant parameter characteristic of the whole froth, and independent of the particular central cell. The dependence of K_j on the number of sides (n) of the central cell can only be an additive constant [i.e., $K_j = Cj + B(n)$]. From a geometrical point of view this additive quantity is associated with the size of the central core made by the first shell and its neighbors. In a system that is uncorrelated after the first shell, the length of the perimeter at shell j is given by the perimeter of this core ($B(n)$) plus a term linearly dependent on the distance (Cj). The generalized Aboav-Weaire relation [Eq. (A2) in Appendix A] gives

$$\langle (6-m_j)K_j \rangle = \langle (6-n)B(n) \rangle \quad \text{for } j \geq \xi. \quad (35)$$

By assuming $\xi = 2$ and using Eq. (32), we obtain

$$\langle (6-m_j)K_j \rangle = \langle (6-n)K_2 \rangle \simeq -(2-a)\mu_2 \quad \text{for } j \geq 2. \quad (36)$$

Equation (36) states that the topological charge contained inside any layer is a constant quantity equal to $-(2-a)\mu_2$. It follows that the total topological charge inside shell j decreases linearly with j,

$$\langle Q_j \rangle = -(2-a)\mu_2 j + \text{const} \quad \text{for } j \geq 1. \quad (37)$$

Note that the total topological charge in the froth must be lower than 12 [31]. Indeed, a froth with charge $Q = 12$ is a closed cellular system which is tiling of a surface topologically equivalent to a sphere. Therefore, from Eq. (37) it follows that the Aboav coefficients must be smaller than or equal to 2 for Euclidean 2D froth with K_2 given by Eq. (32).

In a Euclidean 2D froth, the number of cells per layer grows linearly with slope C asymptotically. Let us suppose that the percentage of defects with respect to the total number K_j of cells in the layers is a constant Λ independent of the topological distance in this limit. Then the number of cells in the shell skeleton must also grow linearly with j [since $\langle K_j^{\text{sk}} \rangle = (1-\Lambda)\langle K_j \rangle$ and $\langle K_j \rangle$ is linear in j]. Equation (20) indicates that $\langle K_j^{\text{sk}} \rangle$ can be linear if the average topological charge associated with the shell skeleton $\langle Q_j^{\text{sk}} \rangle$ is constant. This implies [Eq. (24)]

$$\langle (6-m_j)K_j \rangle = \langle Q_j - Q_{j-1} \rangle$$
$$= \langle Q_j^{\text{sk}} - Q_{j-1}^{\text{sk}} \rangle - \langle \eta_{j+1}K_{j+1}^d - \eta_j K_j^d \rangle$$
$$= (\langle \eta_j K_j^d \rangle - \langle \eta_{j+1}K_{j+1}^d \rangle) \quad \text{for } j \gg 1. \quad (38)$$

By supposing that the parameter $\eta_j = \eta$ is independent of j for large j, using Eq. (38) we obtain

$$\langle (6-m_j)K_j \rangle \simeq -\eta\Lambda(\langle K_{j+1} \rangle - \langle K_j \rangle) = -\eta\Lambda C \quad \text{for } j \gg 1, \quad (39)$$

which predicts that the charge decreases linearly with j with a decrement of $\eta\Lambda C$ per layer. From Eq. (39), using the expression for m_j obtained in Appendix B [Eq. (B1)] valid for layers of cells uncorrelated with the germ cell (in present case for $j > 2$), we obtain

$$m_j = m_j^{\text{un}} = 6 - \frac{\langle (6-n)K_j \rangle}{\langle K_j \rangle} \simeq 6 + \frac{\eta\Lambda C}{Cj + \langle B \rangle} \simeq 6 + \frac{\eta\Lambda}{j}. \quad (40)$$

Supposing that $\langle K_j \rangle$ grows linearly from the second shell (i.e., fixing $\nu = 1$), from Eqs. (31) and (34) we obtain the slope

$$C \simeq \langle K_3 \rangle - \langle K_2 \rangle \simeq 6 + (3-a)\mu_2 - \langle K_2^d \rangle. \quad (41)$$

By comparison between Eqs. (36) and (39), and using expression (41), we obtain an expression for the percentage of defects,

$$\eta\Lambda \simeq \frac{(2-a)\mu_2}{6 + (3-a)\mu_2 - \langle K_2^d \rangle} \simeq \frac{(2-a)\mu_2}{6 + (3-a)\mu_2}, \quad (42)$$

where we assumed $\langle K_2^d \rangle \ll 6 + (3-a)\mu_2$. From Eq. (42) one notes that a froth can be free of defects only if $\mu_2 = 0$ or $a = 2$. The first case ($\mu_2 = 0$) corresponds to the hexagonal lattice, which is SSI and therefore free of defects. The second case ($a = 2$) corresponds to a froth where the Aboav parameter takes the maximum allowed value for a Euclidean froth. This is a very peculiar froth which has a constant topological charge in the shell clusters and does not need defects to fill the plane. So far such a froth has not been observed, to our knowledge. Note that $a = 2$ is a critical value since froths with $a > 2$ are closed elliptic systems. That might suggest that the value $a = 2$ is an upper limit which cannot be reached for Euclidean froths.

In an earlier paper [22], we used the shell model to test a generalization of Aboav-Weaire's law to shells beyond the first. These analyses revealed a universal topological relation on the average number m_j of sides per cell to the number of cells K_j in the jth layer of a given center cell with n sides. A plot of $m_j K_j$ vs K_j shows a slope of $(6-a)$ for $j = 1$ (Aboav-Weaire's law) and a slope of 6 for $j \geq 2$ for all samples. The results are universal for soap froths in the scaling state with different preparations, different times, and different temperatures. With the small $\eta\Lambda$ approximation and Eq. (40), we can now provide a quantitative explanation to the experimental results. The average number of neighbors m_j in layers of cells uncorrelated with the central cell ($j \geq \xi$) is given by Eq. (B1). Multiplying this expression by K_j we have

$$m_j K_j = m_j^{\text{un}} K_j = \left(6 - \frac{\langle (6-n)K_j \rangle}{\langle K_j \rangle} \right) K_j \quad (j \geq \xi). \quad (43)$$

In the asymptotic limit, using the approximations introduced above, we obtain

$$m_j K_j \simeq 6K_j + (2-a)\mu_2 \quad (j \geq \xi), \quad (44)$$

which is the extension of Aboav-Weaire's law to higher shell numbers.

VI. EXPERIMENTAL RESULTS AND COMPARISON WITH THE THEORETICAL PREDICTIONS

The soap froth chamber consists of two 1.6-cm-thick rectangular plexiglass plates separated by a 0.16-cm-thick spacer. The effective working area for the froth is 26.7×36.8 cm^2, which can be filled with more than 20 000 bubbles as the starting condition. Soap bubbles of different sizes are pumped into the chamber through an inlet to create a relatively random froth. The chamber is filled with excess bubbles such that excess fluid can be forced out of the chamber through another outlet after the soap froth has been drained for a few minutes by setting the chamber vertically. Thus the froth has a negligible volume fraction of liquid to air [33]. The chamber is then sealed by closing the inlet and outlet and placed horizontally. A dark field method is used for viewing from above and a high resolution digital charge-coupled device (CCD) camera of 1037×1344 pixels is used to capture the images at different stages of the evolution of the froth. The experiment starts with about 20 000 bubbles, and is about 10 000 in the scaling state defined by the stationary distribution of sides after about 4 h. However, the topological charge becomes stationary at a much later time with about 4000 bubbles. Runs with a similar initial condition have been recorded and only data with stationary topological charge will be reported in this paper.

In order to compare the physical froth with computer-generated ones, we selected two examples of purely geometric constructions. The first one is the Voronoi construction based on random Poissonian points. The second one is based on the Voronoi construction generated by introducing small perturbations to the triangular lattice, so that we mimic the $T1$ transformation in real froth. We label the physical froth by (S), the random Voronoi froth by (V), and the perturbed one by (P). These two geometric constructions are two simple examples of the random froth and slightly ordered froth. The number of cells for these systems are 3206 for (S), 3783 for (V), and 9634 for (P). The values of μ_2 are 1.33 (S), 1.76 (V), and 1.51 (P). They all approximately obey Aboav-Weaire's law, with coefficient a equal, respectively, to 1.27±0.05 (S), 0.69 ± 0.03 (V), and 0.95 ± 0.07 (P).

In Fig. 2 the number of cells per layer K_j is shown as a function of the distance j for soap, and for Voronoi construction on a set of random points in the plane and on a perturbed triangular lattice. For all systems this number increases linearly with the distance with slopes equal, respectively, to 9.45±0.1 (S), 11.0±0.2 (V), and 9.91±0.08 (P). These linear behaviors indicate that these froths are Euclidean. Using expressions for the minimally correlated Euclidean froths
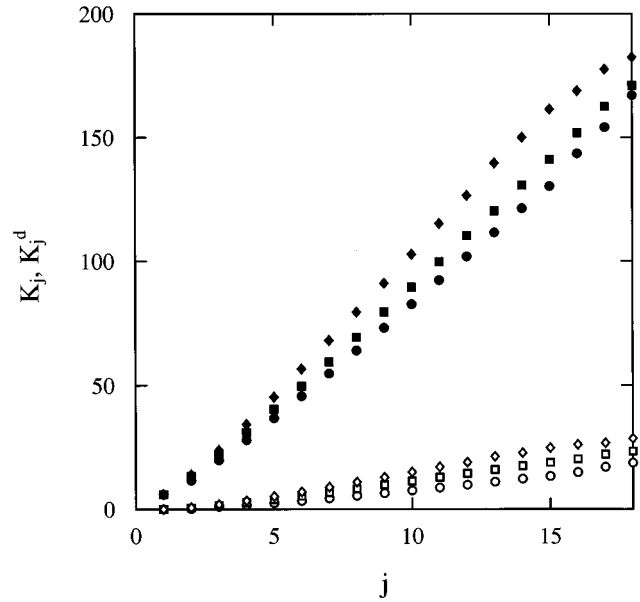
FIG. 2. Total number of cells per layer K_j in the j shell vs shell number j for soap (filled circle), random Voronoi construction (filled diamond), and Voronoi construction from a perturbed triangular lattice (filled square). Total number of defects K_j^d in the jth shell vs j for soap (open circle), random Voronoi construction (open diamond), and Voronoi construction from a perturbed triangular lattice (open square).

obtained in the previous paragraph, one can predict the slopes 8.3±0.3 (S), 10.1±0.4 (V), and 9.1±0.7 (P).

The ratios Λ of the defective cells with respect to the total number of cells in a layer are very small in the second layer [0.0173 (S), 0.05 (V), and 0.05 (P)], then increase until about the 15th layer, to stabilize finally at asymptotic values equal to 0.10±0.01 (S), 0.15±0.01 (V), and 0.13±0.01 (P), respectively. Using expression (42), one can predict for $\eta\Lambda$ the values 0.136 (S), 0.23 (V), and 0.174 (P), respectively. We independently measured the value of η, which gives 1.1±0.2 (S), 1.3±0.1 (V), and 1.2±0.1 (P), respectively. We deduce that the value of defect concentration Λ using these values of η and Eq. (42) are $\Lambda = 0.11 \pm 0.03$ (S), 0.17±0.02 (V), and 0.15±0.03 (P), respectively. This compares reasonably well with the measured values of Λ (see Fig. 3).

Figure 4 shows the total average charge $\langle Q \rangle/\mu_2$ vs j. This quantity decreases with the distance, with an almost linear behavior for $j>2$. The measured slopes are -0.7 ± 0.1 (S), -1.6 ± 0.1 (V), and -1.35 ± 0.05 (P), respectively. Using Eq. (37) one predicts -0.73 ± 0.03 (S), -1.31 ± 0.05 (V), and -1.05 ± 0.07 (P).

The topological charge contained inside the cluster delimited by the generic shell j is an important physical parameter. In the previous paragraph we showed that the quantity associated with the shell-structured skeleton Q_j^{sk} should be constant for Euclidean froths. In Fig. 4, $\langle Q^{\text{sk}} \rangle/\mu_2$ is plotted (open symbols) in function of j for the different froths studied. One can note that in all the systems analyzed the quantity $\langle Q^{\text{sk}} \rangle/\mu_2$ saturates at a value equal to about -2.0 ± 0.5 (S), -2.0 ± 0.2 (V), and -1.8 ± 0.2 (P). The saturation val-
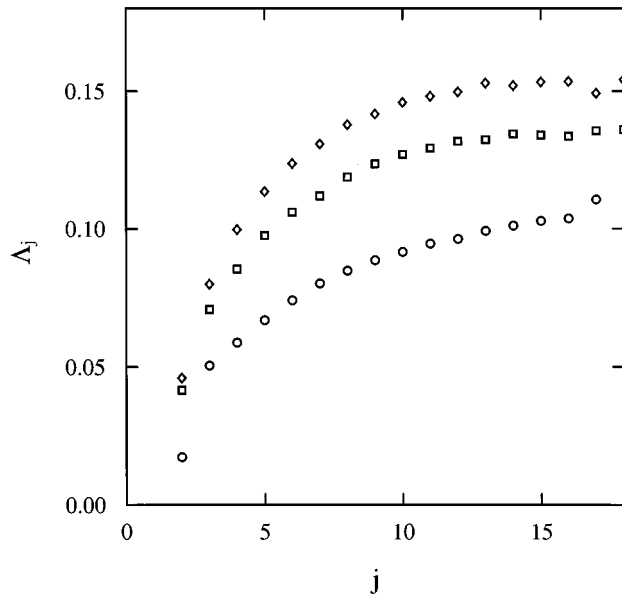
FIG. 3. Defect concentration Λ_j vs shell number j for soap (open circle), random Voronoi construction (open diamond), and Voronoi construction from a perturbed triangular lattice (open square).

ues should be similar for all three cases as $\langle Q^{\text{sk}} \rangle / \mu_2$ is a characteristic of the SSI skeleton.

VII. CONCLUSIONS

We studied froth as organized in concentric layers of cells around a given central cell. Exact expressions for the number of cells in each layer, for the topological charge inside the shell cluster and for the average number of neighbors per cell in a given layer were obtained. These topological properties of the shell structure were studied for the special class of SSI froths and for the general case where non-SSI defects are present. It turns out that the defects play a very important role in the organization of the froth structure. The defects enlarge the freedom for the construction of the cellular system around the germ cell by removing the constraints on the topological charge associated with Euclidean froths. With the relaxation of the constraints by the introduction of defects, we find a solution of space-filling Euclidean froth which has only nearest-neighbor correlations. In this solution, we calculated approximate asymptotic expressions for K_j, Q_j, and m_j which satisfy the Aboav relation and which are correlated only between first neighbors. Moreover, we evaluated the average number of defects per layer. These expressions are free of adjustable parameters, and describe well the behaviors of measurable properties of real froths and cellular patterns.

Experimentally we find that soap froth in the steady state has an average number of cells per layer which grows linearly with the topological distance. The rate of growth is about 9. Slopes of around 10 have been found for Voronoi froths. These slopes are considerably larger than the 2π value suggested by a simple geometrical consideration for the ratio between the perimeter of the shell cluster and its radius. Moreover, we found that in soap and Voronoi froths the topological charge of the shell cluster is always negative
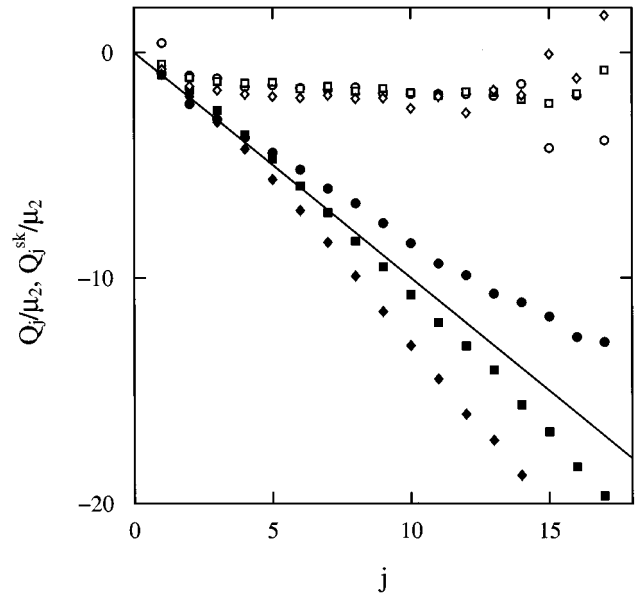
FIG. 4. Normalized cluster topological charge Q_j / μ_2 vs shell number j for soap (filled circle), random Voronoi construction (filled diamond), and Voronoi construction from a perturbed triangular lattice (filled square). The straight line indicates the slope -1. Soap and computer-generated froths are on opposite sides of this line. Normalized cluster topological charge of the skeleton, Q_j^{sk} / μ_2 vs shell number j for soap (open circle), random Voronoi construction (open diamond), and Voronoi construction from a perturbed triangular lattice (open square). Note that the normalized topological charge for the skeleton saturates at about the same value for all cases.

and decreases linearly with the size of the cluster. In particular, we observed that the slope is proportional to $-\mu_2$, and the coefficient of the proportionality is smaller than 1 in soap froths and larger than 1 in computer-generated froths. The number of defects per layer has also been measured. Soap froths in the asymptotic limit have a percentage of defects around 10%, whereas larger amounts were found for computer-generated froths.

Our theory on asymptotic behaviors is in good qualitative agreement with experiments. We correctly predict the linear growth of the number of cells per layer with a slope around 9. We demonstrate the linear decrement in the topological charge of the shell cluster with a slope above the line defined by $-\mu_2$ in soap froths, and with a slope below the line defined by $-\mu_2$ in Voronoi froths. We also predict percentages of defects per layer which are close to the experimental values and are smaller in soap froths and larger in Voronoi froths.

On the other hand, the quantitative agreement between the approximated predictions and the experimental data is not perfect. In the present paper we obtained exact relations for the topological properties of the shell structure, but the predictions were formulated under strong assumptions which simplify the exact results into expressions with no adjustable parameters. The partial disagreement between the approximated predictions and the experimental data might indicate that the assumptions utilized are too strong or incorrect. Therefore there is still room for improvement.

APPENDIX A: GENERALIZATION OF WEAIRE'S SUM RULE

Consider an i cell of the froth with n_i sides, and a sum over the number of sides of the set of cells at a topological distance j from the i cell. Such a sum is equal to $m_j(n_i)K_j(n_i)$, where $m_j(n_i)$ denotes the average number of sides per cell in the layer distant j from the i cell, and $K_j(n_i)$ the number of cells of this layer. Let us now sum this quantity over all the cells of the system: $\Sigma_i m_j(n_i)K_j(n_i)$. In this sum the number of edges of each i cell of the froth is counted a number of times equal to the number of cells at distance j from this cell [e.g., the number of sides of the generic i cell is counted $K_j(n_i)$ times and contributes to the sum as $n_i K_j(n_i)$]. It follows that we have the identity

$$\sum_i m_j(n_i)K_j(n_i) = \sum_i n_i K_j(n_i). \qquad \text{(A1)}$$

We can express this identity in term of the averages

$$\langle m_j K_j \rangle = \langle n K_j \rangle, \qquad \text{(A2)}$$

where $\langle () \rangle$ indicates the average over the cell-side distributions: $\langle () \rangle = \Sigma_n p(n)()$ with $p(n)$ probability of an n-sided cell.

Equation (A2) is the generalization to the layer j of the Weaire sum rule which is valid for the first layer (i.e., $\langle m_1 n \rangle = \langle n^2 \rangle$). For an arbitrarily large system (arbitrary small boundary effects), relation (A2) is exact, and is also valid in the presence of non-shell-reducible topological inclusions. One should note that in real finite systems the effect of the boundary could be dramatically important.

APPENDIX B: CORRELATION AND FLUCTUATIONS

A froth is uncorrelated after a given topological distance ξ if and only if for two cells with distant $j > \xi$, the probability $C_j(n,m)$ to have one with n sides and the other with m sides factorizes $C_j(n,m) = s_j(n)s_j(m)$. It can be easily proved that in a froth where the cells are uncorrelated after the distance ξ, the average number of sides per cell (m_j^{un}) in a layer $j > \xi$ must be independent of the number of sides of the central cell. This is the physical consequence of the absence of correlations between the central cell and the cells in the layer j. This therefore means $\langle m_j^{\text{un}} K_j \rangle = m_j^{\text{un}} \langle K_j \rangle$. By using relation (A2), we have

$$m_j = m_j^{\text{un}} = \frac{\langle n K_j \rangle}{\langle K_j \rangle} = 6 - \frac{\langle (6-n)K_j \rangle}{\langle K_j \rangle} \quad (\text{for } j > \xi). \quad \text{(B1)}$$

The topological charge inside layer j is

$$Q_j - Q_{j-1} = (6 - m_j)K_j = \langle (6-n)K_j \rangle + \Gamma_j - \Gamma_{j-1}. \qquad \text{(B2)}$$

The second equality comes from Eq. (A2). For $j > \xi$, we put Eq. (B1) into Eq. (B2) to obtain, for the uncorrelated case, the relation

$$\Gamma_j = \Gamma_{j-1} + \langle (6-n)K_j \rangle \left(\frac{K_j}{\langle K_j \rangle} - 1 \right) \quad (\text{for } j > \xi). \quad \text{(B3)}$$

This is a recursive equation for the fluctuations Γ_j. Therefore, in uncorrelated froths the topological charge fluctuations are determined in terms of the other statistical properties of the shell system.

Consider, for example, a froth which is completely uncorrelated (topological gas $\xi = 0$). From Eq. (B3), one obtains

$$\Gamma_1 = \left(1 + \frac{\mu_2}{6} \right)(6-n), \qquad \text{(B4)}$$

where we used the identities $K_1 = n$ and $\Gamma_0 = 6 - n$. This relation gives Aboav-Weaire's law [$\Gamma_1 = (1-a)(6-n)$; see text] with a coefficient $a = -\mu_2/6$.

APPENDIX C: PROOF OF THE CORRELATION THEOREM OF EUCLIDEAN SSI FROTH

To prove this theorem, we first note that Eq. (5) implies

$$\langle K_j \rangle = 6j - \sum_{i=0}^{j-1} \langle Q_i \rangle. \qquad \text{(C1)}$$

In order to fill the two-dimensional Euclidean space, there must be a minimum ν such that $\langle K_j \rangle \propto j$ for $j \geqslant \nu$. This implies that the cellular system must constrain the average topological charge inside a shell to be independent on the shell size j. Such a constraint forces the average charge inside the layer j to be equal to zero for $j \geqslant \nu \geqslant 1$ [see Eq. (13)],

$$\langle Q_j \rangle - \langle Q_{j-1} \rangle = \langle (6 - m_j)K_j \rangle$$

$$= -\sum_{i=0}^{j-1} \langle (6-n)\Gamma_i \rangle$$

$$= -\mu_2 - \sum_{i=1}^{j-1} \langle (6-n)\Gamma_i \rangle = 0. \qquad \text{(C2)}$$

Consequently, one obtains the following two conditions on the fluctuations Γ_i:

$$\sum_{i=1}^{\nu-1} \langle (6-n)\Gamma_i \rangle = -\mu_2 \quad \text{for } \nu \geqslant 1, \qquad \text{(C3)}$$

and

$$\langle (6-n)\Gamma_j \rangle = 0 \quad \text{for } j \geqslant \nu. \qquad \text{(C4)}$$

In Appendix B we showed that in a system where the topological correlations vanish after the ξth layer, the fluctuations must satisfy the following relation for $j > \xi$ [Eq. (B3)]:

$$\langle(6-n)\Gamma_j\rangle=\langle(6-n)\Gamma_{j-1}\rangle+\frac{\langle(6-m_j)K_j\rangle^2}{\langle K_j\rangle}. \quad (C5)$$

If one supposes $\nu>\xi$ and if we set $j=\nu$ in Eq. (C5), Eqs. (C2) and (C4) yield $\langle(6-n)\Gamma_{\nu-1}\rangle=0$ which is in contradiction with the definition of ν (for $\mu_2\neq0$). This implies $\nu\leq\xi$. An immediate consequence is that in a random SSI froth where Aboav-Weaire's law is satisfied with an arbitrary a [i.e., $\Gamma_1=(1-a)(6-n)$, for some general a], the cells must be correlated at least between third neighbors. Indeed, $\nu=1$ in Eq. (C4) implies $(1-a)\mu_2=0$, or $a=1$ if $\mu_2\neq0$, whereas $\nu=2$ in Eq. (C3) implies $(1-a)\mu_2=-\mu_2$, or $a=2$ if $\mu_2\neq0$. Both cases restrict a to special values for $\mu_2\neq0$. It follows that if a is to remain a free parameter of the froth, $\nu\geq3$. Since we have shown that $\xi\geq\nu$, therefore $\xi\geq3$.

[1] D. Weaire and N. River, Contemp. Phys. **25**, 59 (1984).

[2] J. Stavans, Rep. Prog. Mod. Phys. **56**, 733 (1993).

[3] J. A. Glazier and J. Stavans, Phys. Rev. **A40**, 7398 (1989).

[4] J. A. Glazier and D. Weaire, J. Phys. Condens. Matter. 4, 1867 (1992).

[5] J. A. Glazier, S. P. Gross, and J. Stavans, Phys. Rev. A **36**, 306 (1987).

[6] J. Stavans and J. A. Glazier, Phys. Rev. Lett. **62**, 1318 (1989).

[7] J. Stavans, Phys. Rev. A **42**, 5049 (1990).

[8] J. Stavans, Physica A **194**, 307 (1993).

[9] J. A. Glazier, M. P. Anderson, and G. S. Grest, Philos. Mag. B **62**, 615 (1990).

[10] E. A. Holm, J. A. Glazier, D. J. Srolovitz, and G. S. Grest, Phys. Rev. A **43**, 2662 (1991).

[11] T. Herdtle and H. Aref, J. Fluid Mech. **241**, 233 (1992).

[12] J. Wejchert, D. Weaire, and J. P. Kermode, Philos. Mag. B **53**, 15 (1986).

[13] D. Lewis, Anat. Rec. **38** 351 (1928).

[14] J. von Neumann, *Metal Interfaces* (American Society for Metals, Cleveland, OH, 1952), p. 108.

[15] D. A. Aboav, Metallography **3**, 383 (1974); **13**, 43 (1980).

[16] D. Weaire, Metallography **7**, 157 (1974).

[17] N. Rivier, Philos. Mag. B **52**, 795 (1985); Physica D **23**, 129 (1986).

[18] J. R. Iglesias and Rita M. C. de Almeida, Phys. Rev. A **43**, 2763 (1991).

[19] J. Stavans, E. Domany, and D. Mukamel, Europhys. Lett. **15**, 479 (1991).

[20] H. Flyvberg, Phys. Rev. E **47**, 4037 (1993); Physica A **194**, 298 (1993).

[21] T. Aste, K. Y. Szeto, and W. Y. Tam (unpublished).

[22] K. Y. Szeto and W. Y. Tam, Phys. Rev. E **53**, 4213 (1996).

[23] W. Y. Tam and K. Y. Szeto, Phys. Rev. E **53**, 877 (1996).

[24] K. Y. Szeto and W. Y. Tam, Physica A **221**, 256 (1995).

[25] M. A. Fortes and P. Pina, Philos. Mag. B **67**, 263 (1993).

[26] R. Delannay and G. Le Caer, Phys. Rev. Lett. **73**, 1553 (1994).

[27] G. Le Caer, J. Phys. A **24**, 1307 (1991).

[28] M. A. Peshkin, K. J. Strandburg, and N. Rivier, Phys. Rev. Lett. **67**, 1803 (1991).

[29] C. Godreche, I. Kostov, and I. Yekutieli, Phys. Rev. Lett. **69**, 2674 (1992).

[30] T. Aste, D. Boose, and N. Rivier, Phys. Rev. E **53**, 6181 (1996).

[31] M. O. Magnasco, Philos. Mag. B **69**, 397 (1994).

[32] T. Aste and N. Rivier, J. Phys. A **28**, 1381 (1995).

[33] F. Bolton and D. Weaire, Phys. Rev. Lett. **65**, 3449 (1990); Philos. Mag. B **63**, 795 (1991).

[34] P. M. Oliveira, M. A. Continentino, and E. V. Anda, Phys. Rev. B **29**, 2808 (1984); B. K. Southern, A. A. Kumar, P. D. Loly, and M-A. S. Tremblay, *ibid.* **27**, 1405 (1983); D. A. Lavis, B. W. Southern, and S. G. Davinson, J. Phys. C **18**, 1387 (1985).

[35] N. Rivier and T. Aste, in *The Geometry of Curved Surfaces and Interfaces*, edited by A. L. Maclay (The Philosophical Transaction A of the Royal Society, London, 1996), Vol. 354, No. 1715, pp. 2055–2069.

[36] V. E. Fradkov, L. S. Shvindlerman, and D. G. Ulder, Philos. Mag. Lett. **55**, 289 (1987).

[37] G. Le Caer and R. Delannay, J. Phys. A **26**, 3931 (1993).